Cement & Concrete Composites 40 (2013) 48–58

Contents lists available at SciVerse ScienceDirect

Cement & Concrete Composites

journal homepage: www.elsevier.com/locate/cemconcomp

A numerical recipe for modelling hydration and heat flow in hardening concrete

Enzo Martinelli [a], Eduardus A.B. Koenders [b,c,*], Antonio Caggiano [d]

[a] DICiv, University of Salerno, Italy
[b] COPPE-PEC – Federal University of Rio de Janeiro, Brazil
[c] Microlab, Delft University of Technology, The Netherlands
[d] LMNI, Intecin/CONICET, FIUBA, University of Buenos Aires, Bs.As., Argentina

ARTICLE INFO

Article history:
Received 14 August 2012
Received in revised form 6 April 2013
Accepted 8 April 2013
Available online 18 April 2013

Keywords:
Heat
Hydration
Cement
Arrhenius
Temperature
Strength

ABSTRACT

This paper presents a sound theoretical formulation and an effective numerical implementation of a heat-flow and hydration model for concrete hardening. The model is based on the Fourier equation of heat flow with the adiabatic hydration curve employed as a reference for simulating the hydration heat source. The proposed formulations are based on a consistent scheme for the partial differential equation and its boundary and starting conditions. The hydration kinetics is simulated through the Arrhenius approach. Formulations for the compressive strength and the elastic modulus are provided and the maturity function is also considered. A finite difference numerical solution is derived with a forward explicit time integration in the time–space domain. The numerical solution is designed as a stepwise "recipe" specifically conceived to be easily implemented by means of either a high-level programming language or even a spreadsheet tool. Experimental temperature measurements for two different mixtures, under adiabatic and semi-adiabatic conditions, are used for validating the proposed model. The adiabatic and semi-adiabatic temperature simulations show good agreement with the experimental data for both concrete mixtures. The degree of hydration could be simulated and used as the fundamental parameter for scrutinising the evolution of the compressive strength. Particularly, a linear trend between the compressive strength and the degree of hydration and the maturity was figured out.

1. Introduction

With the enhanced use of alternative binders and aggregates in sustainable concretes, fundamental material properties will be affected and a change in the performance and response of structural systems can be potentially expected [1]. Partial replacing of classical binders such as Portland cement with sustainable alternatives like granulated slag, fly-ash, rise husk ash, sugarcane bagasse ash, and others, will change the fundamental chemical/physical/mechanical properties of the cementitious microstructure [2]. If besides this, the aggregates will be replaced by a sustainable alternative as well, such as for example aggregates produced from recycled concrete, the concrete will potentially show a different structural performance [3].

A way to evaluate the altered performance of a sustainable concrete is by scrutinising its hardening behaviour in more detail [4]. Particularly, the key aspects of the actual hydration mechanisms [5] can be observed by monitoring the so-called *degree of hydration* of concrete [6,7] and investigating its possible correlations with the development of the relevant material properties, such as compressive strength and elastic modulus [8–11].

As a matter of fact, the degree of hydration can be easily measured only in the case of adiabatic conditions, as in that case it is directly related to the temperature development [6]. On the contrary, in more general conditions, advanced techniques are required to obtain a direct estimate the degree of hydration of concrete during setting and hardening [12–14].

In principle, modern modelling techniques, such as Finite Element (FE) codes with heat transfer and hardening capabilities, can be employed to simulate the temperature development and the hydration process during hardening, within the boarders that these software provide [15,16].

However, a more fundamental approach that can be employed to analyse the early age behaviour of concretes with (partial) replacement of cement and/or aggregates would be to go back to the basic analytical formulations for temperature development and hydration, and to use this as input for the evaluation of the (prevailing) formulae for the development of the material properties [17,18]. This approach gives a deeper insight into the dependency of the material properties on the basic parameters that control the progress of the hydration process. In this way, the

* Corresponding author at: COPPE – Federal University of Rio de Janeiro, Brazil.
E-mail address: e.a.b.koenders@tudelft.nl (E.A.B. Koenders).

0958-9465/$ - see front matter © 2013 Elsevier Ltd. All rights reserved.
http://dx.doi.org/10.1016/j.cemconcomp.2013.04.004

direct correlation between the degree of hydration and the outcome of the formulae for the development of the material properties can be envisioned systematically [8]. Moreover, the possible correlation between the degree of hydration and a simpler parameter, such as the concrete "maturity" can be also proposed.

This paper presents the complete theoretical formulation and a consistent numerical implementation of a model aimed at simulating the cement hydration process and its consequences on the relevant mechanical properties of concrete. Particularly, based on the widely-accepted Arrhenius principle for hydration kinetics [4,6] and the well-established theory of heat flow [19], the proposed model can be considered as a general and handy tool for estimating the degree of hydration from simple temperature measurements carried out during the setting and hardening phases in general non- (or semi-)adiabatic situations. Thus, it could be employed in calibrating sound correlations between material properties, taking into account the effect of concrete mixtures and the possible replacement of Portland cement and aggregates with the by-products mentioned at the beginning of this section. Particularly, unveiling the influence of recycled aggregates and their initial moisture conditions on the final mechanical properties of concrete was the main motivation to develop this model and will be proposed in future stages of the present research.

In this framework, Section 2 outlines the theoretical formulation of the physical/chemical problem under consideration. For the sake of simplicity, and to comply with the aim of the present proposal, such a model is formulated in a 1D space domain and based on assumptions generally accepted at the current state of scientific knowledge. Then, a consistent numerical solution based on the Finite Difference (FD) technique is developed in Section 3 and explained as a "numerical recipe" which is particularly fit for a spreadsheet-based implementation. The experimental results obtained from two concrete mixes are reported in Section 4.1. Since temperature measurements are available for each one of such mixtures in both adiabatic and non-adiabatic conditions, the same experimental results are considered in Section 4.2 to validate the proposed model and demonstrate its ability in simulating the behaviour of hardening concrete in both conditions. The authors are aware that such a model validation would require a much wider set of experimental data; however, the emphasis of the current article is on the theoretical formulation and the numerical implementation (almost a "numerical recipe") of the model, with a focused validation of the simulated results based on a consistent set of experimental data obtained from well-documented research carried out under adiabatic and non-adiabatic conditions. Finally, Section 5 shows a relevant application of the proposed model aimed at unveiling the possible correlation between concrete compressive strength and hydration-related parameters such as degree of hydration and maturity.

2. Theoretical formulation

This section describes the main physical phenomena that occur during concrete setting and hardening and outlines the key theoretical assumptions and the mathematical models currently available to simulate the temperature development and the associated time evolution of the degree of hydration. The main aspects are related to the liberation of heat due to the exothermal nature of the cement hydration reaction. Moreover, the heat-flow developing throughout the hardening concrete specimen as a result of non-adiabatic boundary conditions is analysed to simulate the effect of the variable (semi-adiabatic) temperature development on the cement hydration process and the resulting concrete maturity. Then, the correlations between the hydration process and the progressive development of the relevant mechanical properties of concrete, i.e. the compressive strength and the elastic modulus, are reported.

2.1. Adiabatic heat development of concrete

The chemical reactions which take place during concrete setting and hardening phases are mainly driven by the hydration process of the cement grains within the concrete mix. The cement hydration reaction is exothermic in nature and results in a significant production of heat inside the hardening concrete. The actual status of the cement hydration reaction can be described in terms of the so-called *degree of hydration* $\alpha_h(t)$ which is defined as the ratio between the amount of hydrated cement at time t relative to the original amount of cement in the mix. Since the amount of hydrated cement at time t is proportional to the total amount of heat $Q(t)$, the degree of hydration can be analytically defined as follows:

$$\alpha_h(t) = \frac{Q(t)}{Q_{max}}, \tag{1}$$

where Q_{max} is the amount of heat potentially liberated by the hydration of the total amount of cement actually present in the concrete mix under consideration.

The heat produced by the hydration reaction is significantly influenced by the temperature which depends on the sample dimensions and boundary conditions and, then, is controlled, in turn, by the produced heat itself. Particularly, a simple analytical relationship can be written between the degree of hydration α_h (or the heat $Q_a(t)$ produced in the same conditions) and the corresponding temperature variation ΔT_a in the ideal case of adiabatic conditions [20]:

$$\Delta T_a(t) = \frac{C}{\rho_c c_c} \cdot Q_a(t) = \frac{C \cdot Q_{max}}{\rho_c c_c} \cdot \alpha_h(t), \tag{2}$$

where C is the cement content per unit volume (g/m^3), c_c is the specific heat of concrete (J/g K), and ρ_c is the specific mass of concrete (g/m^3).

Thus, the current temperature developed within the hardening concrete can be expressed by introducing in Eq. (1) the definition of α_h reported in Eq. (2):

$$T_a(t) = T_R + \Delta T_a(t) = T_R + \frac{C \cdot Q_{max}}{\rho_c c_c} \cdot \alpha_h(t), \tag{3}$$

where T_R is the room temperature.

Since the hydration process results in a partial reaction of cement grains which produces the reaction heat denoted as $Q^*_{max} \leqslant Q_{max}$ the following relationship can be introduced between Q^*_{max} and Q_{max} by considering the definition of α_h reported in Eq. (1):

$$Q^*_{max} = Q_{max} \cdot \left[\lim_{t\to\infty} \alpha_h(t)\right] = Q_{max} \cdot \alpha_{h,max}, \tag{4}$$

where $\alpha_{h,max}$ is the degree of hydration theoretically achieved at the end of the hydration process (namely, in the limit for $t \to \infty$). Thus, the degree of hydration in adiabatic conditions (consistently denoted as $\alpha_{a,h}$) can also be expressed in terms of temperature increase:

$$\alpha_{a,h}(t) = \frac{Q_a(t)}{Q_{max}} = \frac{\Delta T_a(t)}{\Delta T_{a,max}} \cdot \alpha_{h,max}. \tag{5}$$

where $\Delta T_{a,max}$ is the asymptotic value achieved by the temperature in adiabatic conditions.

Finally, based on the results of experimental tests on hardening concrete samples in adiabatic conditions, two possible analytical expressions were proposed to approximate the observed time evolution of the hydration heat $Q_a(t)$ [4]:

$$Q_a(t) = Q^*_{max}\left(1 - e^{-rt}\right). \tag{6}$$

$$Q_a(t) = Q^*_{max} \cdot e^{-\left(\frac{\tau}{t}\right)^{\beta}}, \tag{7}$$

where Q^*_{max} is the total heat produced by the hydration reaction in adiabatic conditions and r, τ and β control the shape of the functions introduced to describe the heat evolution in time.

2.2. Heat flow and degree of hydration during setting and hardening

Since concrete is generally cured in non-adiabatic conditions, heat-flow occurs throughout the concrete body during setting and hardening phases and results in a generally non-uniform transient temperature field.

As a matter of principle, the non-stationary heat conduction problem characterising the thermal behaviour of concrete during setting and hardening can be described by the well-known Fourier equation [19]. In the case of the 1D geometry considered in the present study (Fig. 1), such a Partial Differential Equation (PDE) has the following analytical expression:

$$\rho_c c_c \frac{\partial T}{\partial t} = \lambda_c \cdot \frac{\partial^2 T}{\partial x^2} + q_c(x,t), \tag{8}$$

where λ_c is the heat conduction coefficient (W/m K), T is the temperature filed in concrete (K), t is the time (s) and q_c is the rate of heat source (J/m^3 s) and

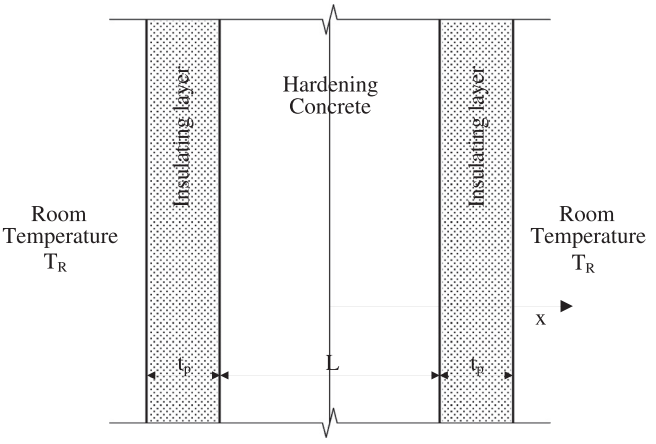

Fig. 1. Geometrical description of the 1D problem.

$$q_c(x,t) = C \cdot \frac{dQ_c}{dt}, \tag{9}$$

where Q_c is the function describing the heat produced by the hydration reaction per unit mass of cement in general (non-adiabatic) conditions.

As already mentioned in Section 2.1, heat source q_c is significantly affected by the actual values of the temperature developed inside the concrete sample. Then, since temperature itself depends on the produced heat, a clear feedback effect can be recognised between q_c and T. Therefore, the effect of absolute temperature T on the rate $V(T)$ of the chemical reaction can be generally expressed through the well-known Arrhenius equation which can be analytically described by the following relationship [4]:

$$V(T) = A_V e^{-\frac{E_A}{RT}}, \tag{10}$$

where A_V is a reference rate value, E_A is the apparent activation energy (usually expressed in J/mol) and R is the universal gas constant ($R \approx 8.3145$ J/mol K). In principle, the values of A_V and E_A can be determined by measuring the rate V under two different temperature values. However, the following applications will be based on assuming $E_A = 33{,}000$ J/mol for hardening concrete, according to experimental results currently available in the scientific literature [21–23].

The Arrhenius equation (10) is useful to express the relationship between the actual heat production rate $q_c(T)$ and the corresponding one $q_a(T_a)$ which should have been measured under adiabatic conditions at the same stage of the hydration reaction (Fig. 2). Thus, if the semi-adiabatic process has achieved the degree of hydration $\alpha_h(t)$ at the time t, an equivalent time t_{eq} can be defined to identify the corresponding status of the hydration reaction in adiabatic conditions:

$$Q_a(t_{eq}) = \alpha_h(t) \cdot Q_{max}. \tag{11}$$

The actual analytical expression of t_{eq} depends on the analytical form chosen for describing the function $Q_a(t_{eq})$. For instance the following two expressions correspond to the two functions reported in Eqs. (6) and (7), respectively:

$$(1 - e^{-rt_{eq}}) = \frac{\alpha_h(t)}{\alpha_{h,max}} \quad t_{eq} = -\frac{1}{r} \cdot \ln\left[1 - \frac{\alpha_h(t)}{\alpha_{h,max}}\right] \tag{12}$$

$$e^{-\left(\frac{\tau}{t_{eq}}\right)^{\beta}} = \frac{\alpha_h(t)}{\alpha_{h,max}} \quad t_{eq} = -\frac{\tau}{\left\{\ln\left[\frac{\alpha_h(t)}{\alpha_{h,max}}\right]\right\}^{\frac{1}{\beta}}} \tag{13}$$

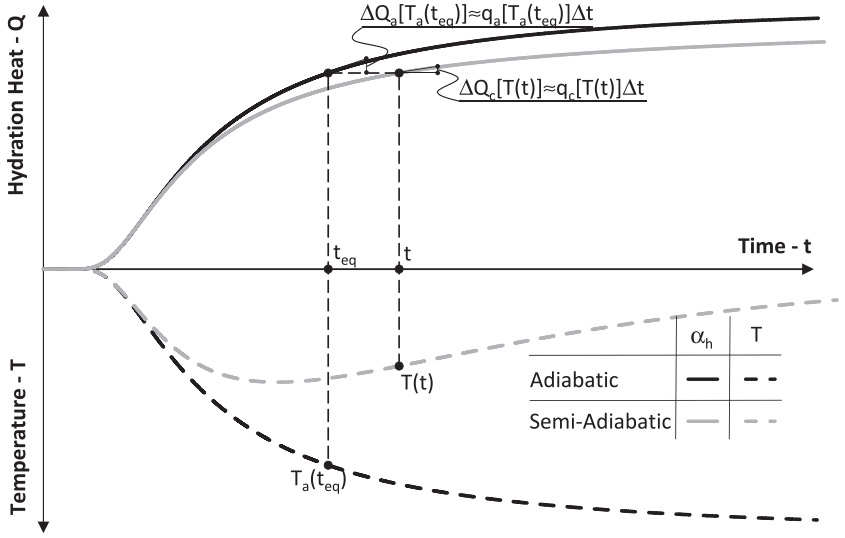

Fig. 2. Hydration heat produced and temperature developed in adiabatic and non-adiabatic conditions.

Although, in principle, the amount of heat $Q_c(T)$ produced by the general hydration process is equal to that correspondingly generated in the ideal adiabatic process up to the time t_{eq}, the two temperatures T and T_a developed in the two systems at time t and t_{eq} are not equal, as a result of the heat transfer phenomena taking place in this respect. Having pointed out this, a clear relationship can be stated through Eq. (10) between the rate of heat production in the two above mentioned conditions:

$$\frac{q_c[T(t)]}{q_a[T_a(t_{eq})]} = \frac{e^{-\frac{E_A}{R\cdot T(t)}}}{e^{-\frac{E_A}{R\cdot T_a(t_{eq})}}} = e^{-\frac{E_A}{R}\frac{T_a(t_{eq})-T(t)}{T_a(t_{eq})\cdot T(t)}}. \tag{14}$$

As clearly demonstrated in [17], the Arrhenius approach is most accurate for concretes whose binder is mainly made of Portland Cement (e.g., CEM I and CEM II according to the European Classification [24]) as a unique dominant reaction phase, i.e. C_3S, can be recognised in such materials. For such materials, the following analytical expression can be determined for the PDE describing the heat flow in hardening concrete by introducing in Eq. (8) the expression of $q_c[T(t)]$ derived by Eq. (14):

$$\rho_c c_c \frac{\partial T}{\partial t} = \lambda_c \cdot \frac{\partial^2 T}{\partial x^2} + q_a[T_a(t_{eq})] \cdot e^{-\frac{E_A}{R}\frac{T_a(t_{eq})-T(t)}{T_a(t_{eq})\cdot T(t)}}. \tag{15}$$

where the flow source in adiabatic conditions can be determined as follows:

$$q_a[T_a(t_{eq})] = C \cdot \left.\frac{dQ_a}{dt}\right|_{t=t_{eq}}. \tag{16}$$

Because of the definition reported in either (12) or (13), Eqs. (15) and (16) leads to a set of integral–differential equations which can be solved numerically, as explained in Section 3, once initial and boundary conditions are defined. Initial conditions are rather simple, as room temperature T_R has to be imposed to the entire space domain at $t = 0$:

$$T(x, t = 0) = T_R. \tag{17}$$

Boundary condition at the two external sides can be directly imposed if the time evolution of temperatures $T_{left}(t)$ and $T_{right}(t)$ measured there during the hydration process are actually available:

$$T(x = -L/2, t) = T_{left}(t), \quad T(x = L/2, t) = T_{right}(t). \tag{18}$$

where L is the characteristic length of the 1D system under consideration. More often, an insulating layer bounds the two external surfaces of the concrete specimen (Fig. 1). If t_p is the thickness of such a layer, and λ_p is its heat conduction coefficient, the boundary conditions can be derived by expressing the continuity of the heat flows $q_{left}(t)$ and $q_{right}(t)$ throughout the insulation-concrete interfaces:

$$q_{left}(t) = \lambda_p \cdot \frac{T_{left}(t) - T_R}{t_p} = \lambda_c \cdot \left.\frac{\partial T}{\partial x}\right|_{x=-\frac{L}{2}}, \tag{19}$$

$$q_{right}(t) = \lambda_p \cdot \frac{T_{right}(t) - T_R}{t_p} = -\lambda_c \cdot \left.\frac{\partial T}{\partial x}\right|_{x=\frac{L}{2}}. \tag{20}$$

Thus, Eq. (15), initial conditions (17) and boundary ones (19) and (20), describe completely the 1D heat-flow occurring within the hardening concrete element describing in Fig. 1.

2.3. Development of the relevant mechanical properties

It is widely recognised that the degree of hydration α_h controls the key relevant mechanical properties of concrete during the hardening phase [4,16,17]. Particularly, for the sake of brevity, only the formulations for two main properties, i.e. the compressive strength f_c and Young Modulus E_c, are provided in this section.

The formulation for the compressive strength development was investigated in-depth and the following linear relationship between f_c and α_h was proposed [8]:

$$f_c = f_{c,max}\frac{\alpha_h - \alpha_0}{1 - \alpha_0}. \tag{21}$$

where $f_{c,max}$ is the fictitious maximum strength in the ideal case of complete hydration ($\alpha_h = 1.0$) and α_0 is the so-called critical hydration below which no relevant strength gain is achieved. It is worth reporting that a similar expression between tensile strength $f_{c,t}$ and degree of hydration of concrete was also proposed [8]. In addition to this, for the Young modulus E_c, the following non-linear expression was proposed to describe its relationship with α_h [25]:

$$E_c = E_{c,0} \cdot \sqrt{\frac{\alpha_h - \alpha_0}{1 - \alpha_0}}. \tag{22}$$

in which $E_{c,0}$ is the fictitious elastic modulus potentially achieved for $\alpha_h = 1.0$ and α_0 has the same meaning defined in Eq. (21). In this article, the formulations for the tensile strength and the Young modulus will not be considered any further.

2.4. The "Maturity" concept

As mentioned in Section 2.1 the degree of hydration can be determined from the actual temperature profile and the adiabatic temperature curve. Therefore, in more general conditions, the solution of a heat-flow problem described by the PDEs outlined in Section 2.2 is required to determine $a_h(t)$. However, a possible definition for an alternative parameter that characterises the state of the hydration process, but is easier to measure in both laboratory and field application, would be worthwhile to provide to designers. This would make it more feasible to apply Eqs. (21) and (22) and predict the actual evolution of the relevant mechanical properties during the concrete hydration process. The so-called "maturity" is a parameter which can possibly be considered to describe the status of the hydration reaction, though its definition is less fundamental than α_h [26]. The Nurse–Saul definition of maturity $M(t)$ represents the measure of the area below the temperature–time curve measured on concrete during setting and hardening (Fig. 3):

$$M(t) = \int_0^t T(\tau) \cdot d\tau. \tag{23}$$

An alternative formulation was also proposed for the Maturity concept that takes into account the influence of temperature variation on the hydration reaction rate. Particularly, the definition proposed in [27] is among the most well-established ones and is also recognised in [28]:

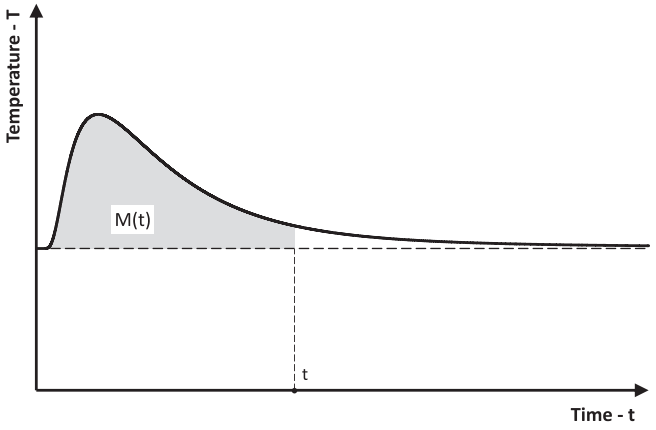

Fig. 3. The graphical interpretation of the Maturity concept.

$$M(t) = \int_0^t T(\tau) \cdot e^{-\left[\frac{E_A}{R}\left(\frac{1}{T_{ref}} - \frac{1}{T(\tau)}\right)\right]} \cdot d\tau, \tag{24}$$

where T_{ref} is an (absolute) reference temperature ($T_{ref} = T_R$ is assumed in this study).

3. Numerical implementation

The set of integral–differential equations described by Eqs. (15) and (16) and the definition of t_{eq} provided by either Eqs. (12) or (13) can be solved numerically through a Finite Difference (FD) approach which is described in Section 3.1. Furthermore, such a solution for the heat-flow problem and the further calculations needed to determine the degree of hydration and associated mechanical properties of concrete is described in detail like a "numerical recipe" described in Section 3.2.

3.1. Finite difference solution

The PDE (15) which describes the heat-diffusion process throughout the hardening concrete can be turned to a convenient FD expression in each node of a time–space mesh. Particularly, the space domain is subdivided in n_s spaces and $(n_s + 1)$ nodes whose distance is

$$\Delta x = \frac{L}{n_s}. \tag{25}$$

Moreover, a time increment Δt is assumed to develop a time-explicit solution scheme. Fig. 4 shows the FD discretisation of the space–time domain and the relevance for the problem under consideration. Then, the FD expression of Eq. (15) is obtained by introducing the central-difference scheme for the space derivative and the forward or backward scheme for the time one. Particularly, the following FD expressions are adopted herein to approximate the second space derivative and the first time derivative of the temperature field $T(x,t)$ in the (n,k)-node of the space–time domain:

$$\left[\frac{\partial^2 T}{\partial x^2}\right]_{n,k} \approx \frac{T_{n+1,k} - 2 \cdot T_{n,k} + T_{n-1,k}}{\Delta x^2}, \tag{26}$$

$$\left[\frac{\partial T}{\partial t}\right]_{n,k} \approx \frac{T_{n,k+1} - T_{n,k}}{\Delta t}, \tag{27}$$

where a forward scheme is assumed for the latter, which leads to an explicit numerical integration scheme. Thus, the following FD algebraic equation can be determined by introducing Eqs. (26) and (27) in (15) in order to express the value $T_{n,k+1}$ of the temperature field in the $(n,k+1)$-node:

$$T_{n,k+1} = T_{n,k} + a_c \cdot \frac{\Delta t}{\Delta x^2} \cdot (T_{n+1,k} - 2 \cdot T_{n,k} + T_{n-1,k}) + \frac{\Delta Q_a\left[T_a(t_{eq,n,k})\right]}{\rho_c c_c} \cdot e^{-\frac{E_A}{R}\left(\frac{T_{a,eq,n,k} - T_{n,k}}{T_{a,eq,n,k} \cdot T_{n,k}}\right)} \tag{28}$$

where n ranges from 1 to $(n_s - 1)$ and

$$a_c = \frac{\lambda_c}{\rho_c c_c} \tag{29}$$

and then $T_{a,eq,n,k}$ is the temperature which would have been developed in adiabatic conditions at the time $t_{eq,n,k}$ defined in Eq. (11), through the analytical expression described by Eqs. (12) and (13) corresponding to the heat production functions (6) and (7), respectively. In fact, it can be determined through Eq. (3) which can be finally expressed as follows, taking into account the Eqs. (6) and (4):

$$T_{a,eq,n,k} = T_a(t_{eq,n,k}) = T_R + \frac{C}{\rho_c c_c} \cdot Q_a(t_{eq,n,k}). \tag{30}$$

Particularly, the definition of $t_{eq,n,k}$ is based on the degree of hydration $\alpha_{h,n,k}$ developed up to the end of the kth step of the forward time integration. It can be evaluated as follows:

$$q_{c,n,k+1} = q_c(T_{n,k+1}) = q_a(T_{a,eq,n,k+1}) \cdot e^{-\frac{E_A}{R} \cdot \frac{T_{a,eq,n,k+1} - T_{n,k+1}}{T_{a,eq,n,k+1} \cdot T_{n,k+1}}}, \tag{31}$$

$$Q_{c,n,k+1} = \sum_{i=1}^{k+1} \frac{q_{c,n,i} + q_{c,n,i-1}}{2} \cdot \Delta t, \tag{32}$$

$$Q_{c,k+1} = \frac{1}{L} \sum_{n=1}^{n_s} \frac{Q_{c,n,k+1} + Q_{c,n-1,k+1}}{2} \cdot \Delta x, \tag{33}$$

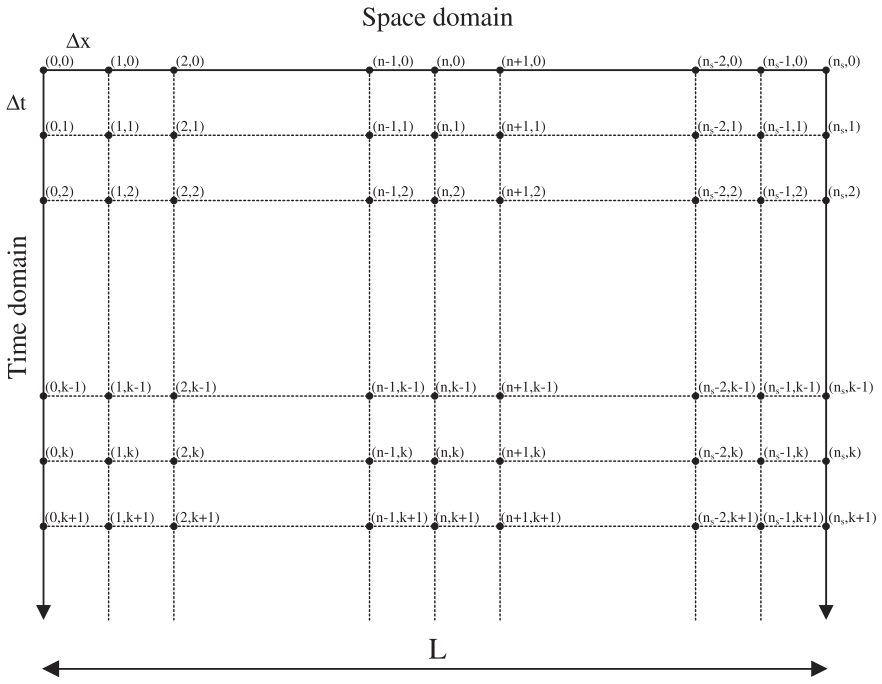

Fig. 4. Finite difference scheme integration in time and space.

$$\alpha_{h,n,k+1} = \frac{Q_{c,n,k+1}}{Q_{max}}, \quad \alpha_{h,k+1} = \frac{Q_{c,k+1}}{Q_{max}} \tag{34}$$

Initial conditions can be easily imposed as follows according to Eq. (17):

$$T_{n,0} = T_R \quad \text{for } n = 0, \ldots, n_s \tag{35}$$

Moreover, boundary conditions in space can be turned into a convenient FD form by transforming the analytical expressions reported in Eqs. (19) and (20):

$$\lambda_p \cdot \frac{T_R - T_{0,k+1}}{t_p} = \lambda_c \cdot \frac{T_{1,k+1} - T_{0,k+1}}{\Delta x}, \quad \Rightarrow T_{0,k+1} = \frac{\frac{\lambda_p}{t_p} \cdot T_R + \frac{\lambda_c}{\Delta x} \cdot T_{1,k+1}}{\frac{\lambda_p}{t_p} + \frac{\lambda_c}{\Delta x}} \tag{36}$$

$$\lambda_p \cdot \frac{T_{n_s,k+1} - T_R}{t_p} = -\lambda_c \cdot \frac{T_{n_s,k+1} - T_{n_s-1,k+1}}{\Delta x} \Rightarrow T_{n_s,k+1} = \frac{\frac{\lambda_p}{t_p} \cdot T_R + \frac{\lambda_c}{\Delta x} \cdot T_{n_s-1,k+1}}{\frac{\lambda_p}{t_p} + \frac{\lambda_c}{\Delta x}}. \tag{37}$$

Eq. (28) demonstrates that the outlined numerical procedure is explicit in space and time, as the value $T_{n,k+1}$ depends on values of the temperature field at time t_k and, through the definition of $t_{eq,n,k}$ (which can be deducted by (12) and (13)), it also involves the degree of hydration $\alpha_{h,n,k}$ at time t_k which, in turn, depends on all previous analysis steps, as a result of the nature of the differential Eqs. (15) and (16). However, for each instant t_k the value of the temperature field in $(n_s + 1)$ nodes should be determined. In fact, $(n_s - 1)$ field Eq. (28) along with the boundary conditions (36) and (37) balance the number of unknowns.

In order to achieve a stable solution for the explicit numerical integration scheme considered in this approach, Eq. (28), a convergence criterion has to be considered. For a steady state 1D schematisation for time integration, the following criterion holds [29,30]:

$$\frac{a_c \cdot \Delta t}{\Delta x^2} \leqslant \frac{1}{2}. \tag{38}$$

Finally, the two definitions of concrete maturity reported in Eqs. (23) and (24) can be easily calculated in the general node n of the space domain on the basis of the numerical values of the time evolution of temperature field $T_{n,k}$:

$$M_n(t) = \sum_{i=1}^{k} \frac{T_{n,i} + T_{n,i-1}}{2} \cdot \Delta t, \tag{39}$$

$$M_n(t) = \sum_{i=1}^{k} \frac{T_{n,i} \cdot e^{-\left[\frac{E_A}{R}\left(\frac{1}{T_{ref}} - \frac{1}{T_{n,i}}\right)\right]} + T_{n,i-1} \cdot e^{-\left[\frac{E_A}{R}\left(\frac{1}{T_{ref}} - \frac{1}{T_{n,i-1}}\right)\right]}}{2}. \tag{40}$$

Then, a global value of such a parameter for the whole specimen can be calculated through a space average:

$$M(t_k) = \frac{1}{L} \cdot \sum_{n=1}^{n_s} \frac{M_n(t_k) + M_{n-1}(t_k)}{2}.$$

3.2. Details about the proposed numerical "recipe"

The proposed numerical solution of the heat-flow problem (Section 3.1) can be easily implemented in either a high-level programming language or a spreadsheet tool. In this second case, each node of the space–time domain represented in Fig. 4 can correspond to a cell of the spreadsheet and the equations can be solved iteratively for each time step. The numerical scheme described by Eq. (28) can be copied in all cells corresponding to the internal nodes of the FD mesh represented in Fig. 4. The boundary conditions in space are created by considering at each time step the Eqs. (36) and (37) on the left and right lateral borders, respectively. The starting conditions of the PDE represent the actual temperature of the concrete mix: this is the temperature directly after mixing and represents the initial condition of the elements $T(x, t = 0) = T_R$. As long as hydration proceeds ($Q_a(t) > 0$), heat will be generated by the adiabatic curve reported in Eq. (7) and the temperature will be transferred to the boundaries according to the heat flow Eq. (28). The continuous increase of heat will lead to an increase of the temperature while the associated temperature field is solved by the spreadsheet solver. From the calculated temperature field the distribution of the degree of hydration can be calculated at the end of the current time step through Eqs. (31), (32), (34). The degree of hydration will depend on the development of the temperature in the different cells and indicate the amount of hydration products that have been formed in the concrete during hydration. Therefore, based on this, the Eqs. (21) and (22) for strength and elastic modulus are implemented, and relate the development of these mechanical properties to the degree of hydration.

Finally, Fig. 5 depicts a flow-chart of the proposed numerical "recipe". It describes the sequence of operations possibly needed to implement the proposed numerical simulation whose time integration ends when the amount of heat produced in the last iteration falls below a given user-defined tolerance represented by

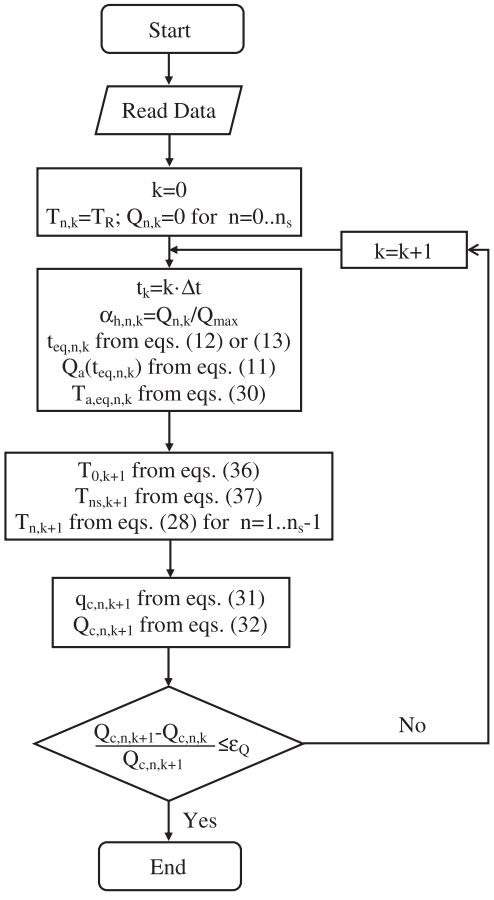

Fig. 5. Flow-chart of the proposed numerical procedure.

the parameter ε_Q reported in the last "diamond" block of the flowchart in Fig. 5.

4. Validation of the proposed heat-flow and hydration model

This section summarises the experimental results considered as a benchmark in this study and proposes the comparison between such results and the corresponding numerical simulations, whose agreement leads to the validation of the proposed model.

4.1. Outline of experimental test setups

The model presented in Sections 2 and 3 needs to be validated in its capability to simulate the hydration process under both adiabatic and non-adiabatic conditions. Experimental data, characterising the hydration process of four concrete mixtures for a water–cement ratio $w/c = 0.4$, was obtained from temperature measurements conducted at Delft University of Technology (The Netherlands) and reported in [20]. However, since the proposed model relies upon the Arrhenius function for controlling the rate of the hydration heat mentioned in Section 2.2, and is, therefore, most accurate for applications with Portland Cement-based concretes [31,32], only the specimens indicated as "Mixture 3" and "Mixture 4" are considered in the present study. Particularly, Mixture 3 contains 450 kg/m^3 of CEM I 32.5 with addition of 5% of silica-fume, and Mixture 4 contains 450 kg/m^3 of CEM IV/A 32.5 R, while both mixtures were mixed with a w/c ratio of 0.4 (Tables 1 and 2). From the experimental data a set of temperature measurements carried out on different concrete samples cured at both adiabatic and non-adiabatic conditions was available [20]. Fig. 6 depicts the experimental equipment employed in the experimental tests.

The adiabatic hydration curve is measured from a freshly cast concrete cube for which the thermal boundary conditions are controlled in such a way that heat liberation to the surrounding is prevented. This means that all heat generated inside the concrete cube will be used in favour of the rate of the chemical reaction process. It is a method to calculate the maximum heat generated by a concrete mixture. At Delft University of Technology, the test set-up to determine the adiabatic hydration curve consists of an insulated mould of which the thermal boundary conditions are controlled by a computer and a cryostat unit (Fig. 6a).

To measure the semi-adiabatic temperature evolution, the dummy setup is used (Fig. 6b), which is part of the Thermal Stress Testing Machine (TSTM), and is generally used to measure temperature developments and free deformations. The temperature evolution is measured in the centre of the specimen, at half of the specimen height; the thickness of the specimen is 100 mm and the width 150 mm (Fig. 6b). The mould is thermally insulated which leads to the increased temperature evolution during hardening (semi-adiabatic).

Compressive strength measurements are obtained from cubic specimen of $150 \times 150 \times 150$ mm^3 [33] and were tested at 1, 3, 7 and 28 days (3 for each age). After casting, the cubes were vibrated and covered with a plastic foil. The semi-adiabatic temperature evolution measured from the test setup (Fig. 6b) was imposed to the compressive strength cubes by means of thermally adaptive cubes to which copper water tubes mounted, at the side panels of the steel moulds (Fig. 6c). A computer was used to adapt the temperature in the compressive strength moulds being equal to the semi-adiabatic temperature evolution using cryostat units.

4.2. Temperature experiments and numerical predictions

To validate the proposed flow and hydration model, both adiabatic and semi-adiabatic temperature evolution measurements are simulated. Fig. 7 describes the time evolution of the temperatures measured in the specimens made of the Mixtures 3 and 4 under the conditions described above. The adiabatic temperature curves show the upper boundaries of the temperature evolution whereas temperature measurements under semi-adiabatic conditions show a maximum after which the temperature turns back to the constant room temperature, as a result of the heat flow. Moreover, Fig. 8 reports the time evolution of cubic compressive strength measured from the concrete specimens made of the same mixtures and cured under the same semi-adiabatic conditions. Both the adiabatic and semi-adiabatic temperature mixtures are simulated with the proposed flow model using the input values given in Table 3. Particularly, the simulation has been carried out by fine-tuning the values of τ and β according to an Inverse Identification Procedure [34]. The results are plotted in Figs. 9 and 10 and the model shows similar temperature evolutions as measured experimentally. In the simulations the adiabatic temperature evolution acts as the heat source (Eqs. (6) and (7)) whereas the semi-adiabatic temperature evolution represents the respond of the model. The potential of the model to simulate the temperature evolutions of Mixtures 3 and 4 under semi-adiabatic conditions with just using their adiabatic temperature curves as the main source for the maximum heat development, is very promising. Figs. 11 and 12 show the space variation of temperature inside the concrete sample after 12, 24 and 48 h of hydration. They clearly

Table 2
Overview chemical composition of CEM I 32.5, CEM IV/A 32.5 R and silica fume.

Component	CEM I 32.5	CEM IV/A (P) 32.5 R	Silica fume
Chemical properties in wt.%			
CaO	64.40	44.3	0.39
SiO_2	20.36	27.8	97.20
Al_2O_3	4.96	5.0	0.51
Fe_2O_3	3.17	5.8	0.18
SO_3	2.57	2.6	0.26
Na_2O	0.14	0.3	–
K_2O	0.64	2.2	1.04
LOI	0.88	3.7	–
Physical properties			
Specific weight (g/cm^3)	3.15	2.98	2.2
Specific surface area	300 m^2/kg	543 m^2/kg	–

Table 1
Overview of mix proportions of Mixtures 3 and 4.

Component	Mixture 3	Mixture 4	Note
Cement	450 kg/m^3	450 kg/m^3	Mixture 3: CEM I 32.5 Mixture 4: CEM IV/A (P) 32.5 R
Silica fume slurry	33.7 kg/m^3	–	Silica mass 5% of cement weight
Sands 0–4	748.1 kg/m^3	738.5 kg/m^3	Based on dry materials
Gravels 4–16	991.7 kg/m^3	978.7 kg/m^3	Based on dry materials
w/c Ratio	0.4	0.4	
Plasticizer	4.95 kg/m^3 (1.1%)	8.1 kg/m^3 (1.8%)	Cugla SL 01 concentration 35%

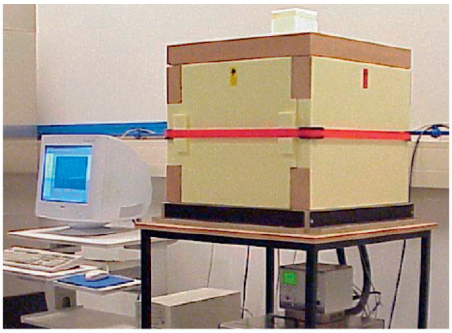

(a) Adiabatic conditions

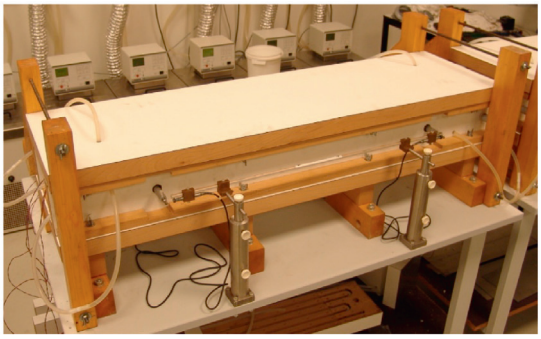

(b) Semi-adiabatic conditions

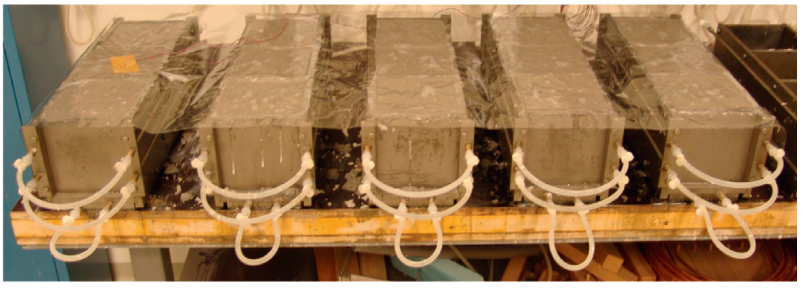

(c) Thermal adaptive moulds formeasuring the compressive strength

Fig. 6. Experimental equipment [20].

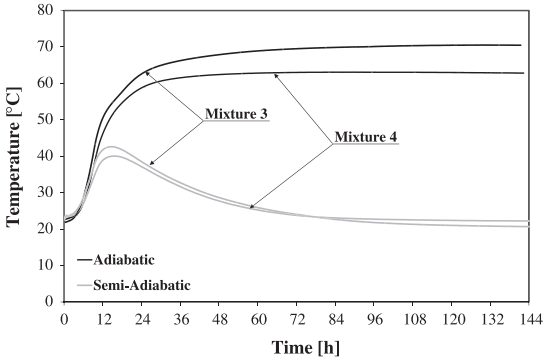

Fig. 7. Experimental results: time evolution of temperature [27].

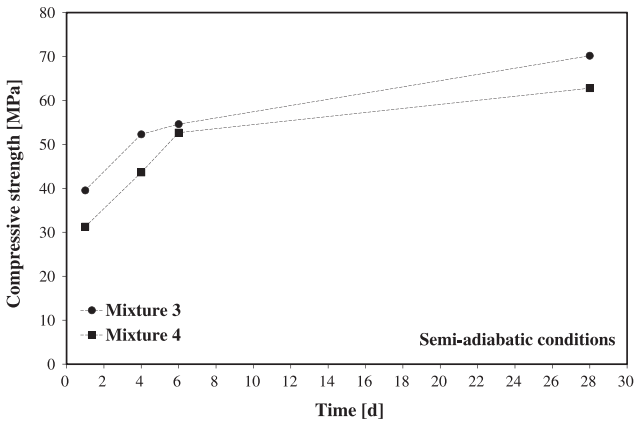

Fig. 8. Experimental results: time evolution of the compressive strength [27].

highlight the heat flow that occurs due to the semi-adiabatic boundary conditions.

From the semi-adiabatic temperature evolution and the adiabatic curve the actual heat flow can be calculated. For this, the actual rate of hydration can be attained by applying the Arrhenius function. This approach enables the calculation of the actual rate of hydration for a (semi-adiabatic) temperature, which is always lower than the adiabatic temperature evolution. From the actual heat development and the maximum heat that can be generated under adiabatic conditions, both degree of hydration and maturity. This approach can also be easily implemented in the numerical solutions (e.g. developed in a spreadsheet) and the evolution of the degree of hydration with time is simulated for both Mixtures

Table 3
Overview of input values used to simulate Mixtures 3 and 4.

Input value flow model	Symbol	Mixture 3	Mixture 4
Maximum degree of hydration (–)	$\alpha_{h,max}$	0.78	0.77
Maximum potential heat (kJ/kg)	Q_{max}	350	300
Cement content (kg/m^3)	C	450	450
Density times specific heat (kJ/m^3 K)	$\rho_c c_c$	2500	2500
Heat conduction coefficient (W/m K)	λ_c	2.5	2.5
Heat diffusion coefficient (m^2/s K)	a_c	1E−6	1E−6
Time increment (s)	Δt	20	20
Space increment (m)	Δx	0.0075	0.0075
Insulation thickness (m)	t_p	0.04	0.04
Heat conduction coefficient of insulation layer (W/m K)	λ_p	0.125	0.125
Apparent activation energy (J/mol)	E_A	33,000	33,000
Universal gas constant (J/mol K)	R	8.31	8.31
Coefficient for adiabatic function (h) acc. to Eq. (6)	τ	8.5	9
Coefficient for adiabatic function (–) acc. to Eq. (6)	β	1.6	2.1

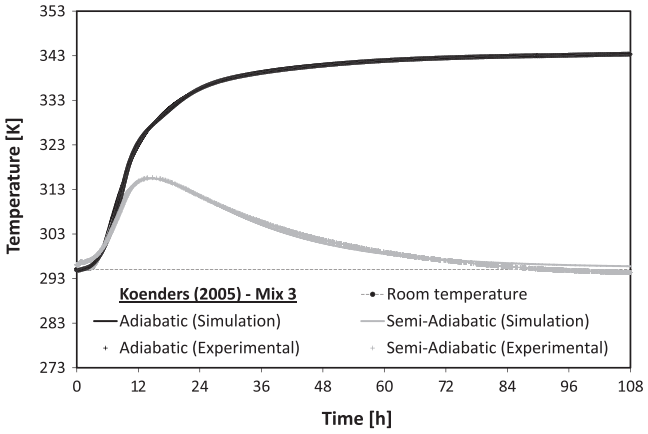

Fig. 9. Time evolution of temperature (adiabatic heat production according to Eq. (7)): Mixture 3.

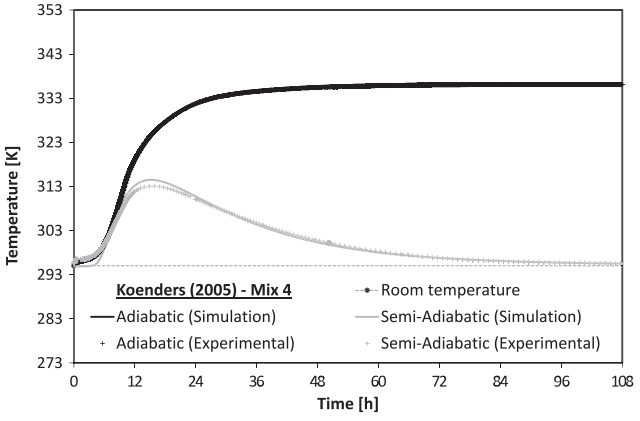

Fig. 10. Time evolution of temperature (adiabatic heat production according to Eq. (7)): Mixture 4.

3 and 4. The results of this calculation are depicted in Figs. 13 and 14. From the results it can be observed that the degree of hydration for both mixtures starts to deviate from hydration under adiabatic conditions at the moment that the temperature evolution is deviating significantly from the adiabatic conditions. The reduced temperature leads to a reduction in the rate of hydration, according to the Arrhenius principle, that finally leads to a lower degree of

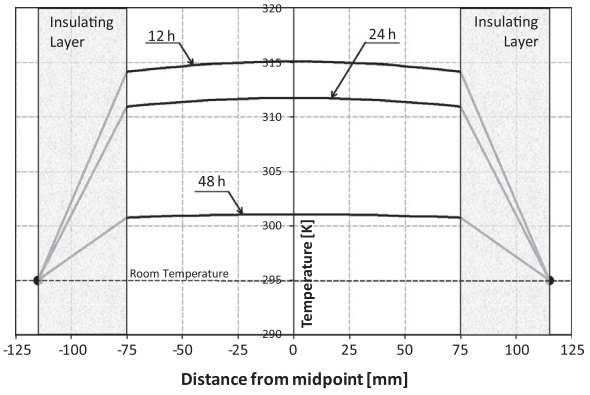

Fig. 11. Space variation of the temperature field at different curing time Mixture 3.

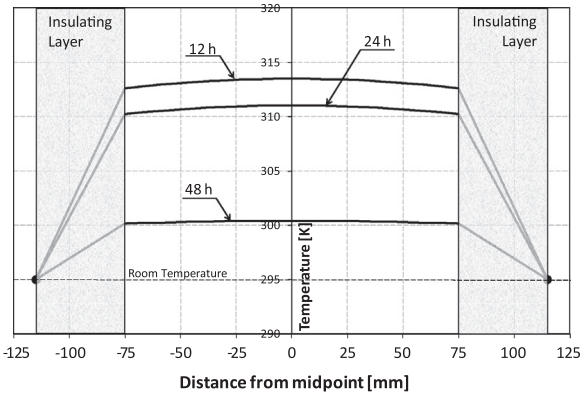

Fig. 12. Space variation of the temperature field at different curing time Mixture 4.

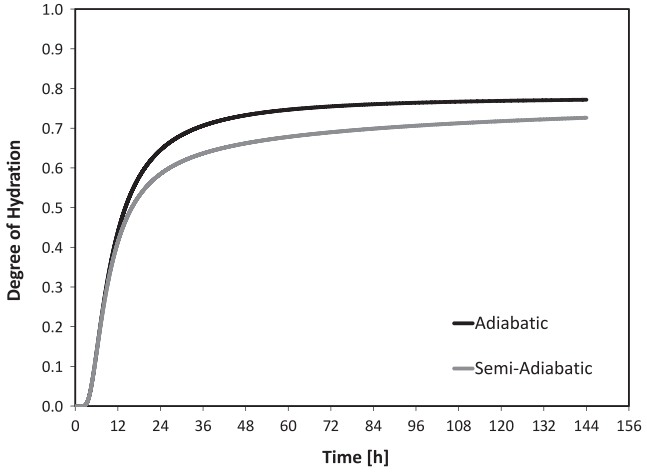

Fig. 13. Time evolution of degree of hydration: Mixture 3.

hydration. However, for the given temperature conditions, the degree of hydration of both mixtures tends to approach the corresponding value achieved in adiabatic conditions closely.

5. Hydration process and material properties

This section outlines a potential application of the proposed model aimed at investigating the possible correlation between the development of concrete compressive strength in the hardening stage and the corresponding status of the cement hydration

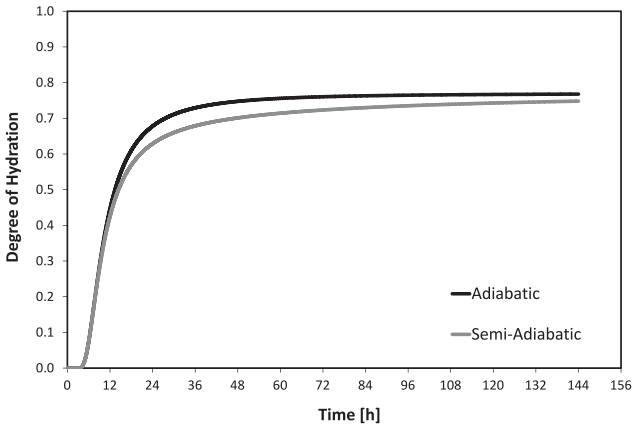

Fig. 14. Time evolution of degree of hydration: Mixture 4.

reaction which can be described in terms of either degree of hydration or maturity. With this, authors have the intension to show the potential of the proposed model in investigating such a fundamental correlation, whose final quantitative definition should be based on a wider set of experiments in terms of both temperature development and concrete strength during the hardening phase.

5.1. Correlation between degree of hydration and compressive strength

As the degree of hydration reflects the amount of cement that has reacted and the progressive formation of a load bearing microstructure that is built up from hydration products, a correlation with the material properties can be expected. In [7–10], several authors reported a strong relationship between the degree of hydration and the compressive strength, the tensile splitting strength and the elastic modulus. In order to evaluate the performance of the flow model and to examine the relationship between the concrete compressive strength and the degree of hydration, the compressive strength tests (Fig. 8) were correlated to the corresponding degree of hydration for both Mixtures 3 and 4. The conceptual results of Fig. 15 emphasise that the number of available data points is not sufficient to be able to confirm a strong correlation between compressive strength and degree of hydration for the Mixtures 3 and 4; however, the potential of the proposed procedure as a fundamental tool to investigate the mechanical properties of concrete clearly emerged, and is in line with the findings reported [7–10].

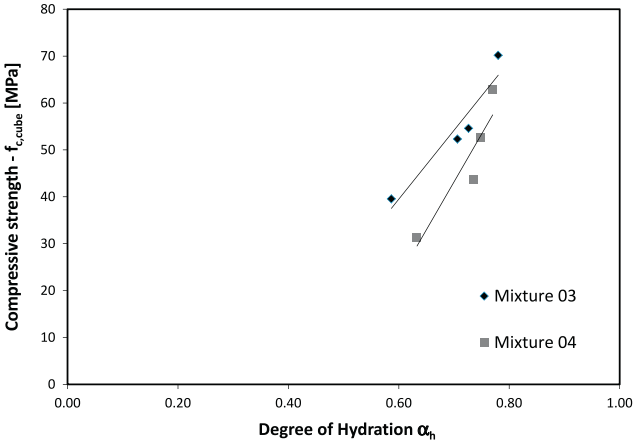

Fig. 15. Correlation between the simulated degree of hydration and the corresponding experimental values of the cube compressive strength (Mixtures 3 and 4).

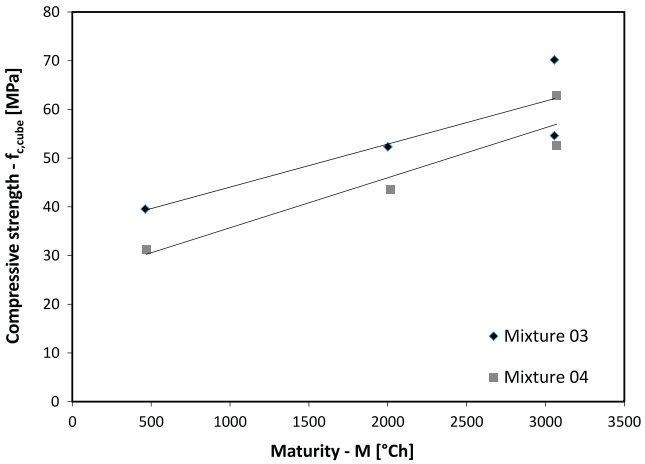

Fig. 16. Correlation between the simulated maturity and the corresponding experimental values of the cube compressive strength (Mixtures 3 and 4).

5.2. Correlation between maturity and compressive strength

A more practical parameter that can be applied to indicate the evolution of the material properties is the maturity (see Section 2.4). When considering the maturity to reflect the state of the hydration process, a correlation between the evolution of the maturity and the compressive strength is also to be expected. In Fig. 16, the evolution of the compressive strength is shown as a function of the maturity. In order to evaluate the linearity of the dependency with the maturity, a trend line was drawn through the available data points as well. The results show a linear correlation where only at the end of hydration the trend becomes more irregular. However, it is worth highlighting that, also for these results, the number of available data points is insufficient to confirm the validity of the proposed trend of this research.

6. Conclusions

This paper proposed a theoretical model for simulating heat and hydration in hardening concrete. A step-by-step "recipe" was presented to make reasonably feasible the numerical implementation of the complex theoretical formulations needed to accurately analyse the above mentioned phenomena. Thus, the model can be easily employed for analysing the evolution of mechanical properties such as the compressive strength, the tensile strength and the elastic modulus, and enables the possibility to relate the development of these material properties to one fundamental parameter, namely the *degree of hydration*. With this, the paper presents a novel method to correlate the development of the mechanical properties to the actual state of the hydration process by simply using the measured temperature development as an indication for the time evolution of the hydration reaction.

Furthermore, the model is validated by means of temperature curves measured from two different hardening concretes under adiabatic and semi-adiabatic conditions. The main aim of this validation is to demonstrate the potential of the proposed method to simulate both the adiabatic hydration curve (heat source) and the semi-adiabatic temperature response (output of the proposed procedure), for given boundary and initial conditions. For the two selected mixtures, good agreement could be found between measured and simulated temperatures. Based on the assumptions of applicability of the Arrhenius principle for concrete, the heat of hydration could also be simulated under general semi-adiabatic conditions, and from this the degree of hydration. The following conclusions can be drawn out:

- The proposed numerical model accurately simulates the temperature evolution of hardening concrete.
- The model simulates the degree of hydration of a hardening concrete sample under adiabatic and semi-adiabatic conditions.
- A correlation between the experimental values of compressive strength and the simulated degree of hydration clearly emerged: however, more data are needed to confirm this observation.
- The correlation between the maturity and the experimentally obtained compressive strength data shows a linear trend: also here, more data are needed to better define such a correlation.
- The proposed 1D flow and hydration model turns out to be a useful tool for researchers to analyse the data obtained from early age concrete problems.

The proposed flow model is developed within the framework of the "EnCoRe" Project and should be considered as a first step towards the design of an analysis tool for concretes with recycled aggregates and binders. The model will be further developed in this respect with emphasis on the mechanical performance of the natural and recycled aggregates partly in combination with replaced binders such as fly-ash. Of particular attention will be the correlation between the evolution of the degree of hydration and the development of the material properties.

Acknowledgements

The present study was mainly developed in the months between April and September 2012, as part of the activities carried out by the Authors within the "EnCoRe" Project (FP7-PEOPLE-2011-IRSES n. 295283; www.encore-fp7.unisa.it) funded by the European Union within the Seventh Framework Programme. Particularly, it began during the visit of the second and third co-authors at the University of Salerno (Italy) and was completed during the first author's secondment at the Federal University of Rio de Janeiro (Brazil).

References

[1] Naik TR. Sustainability of cement and concrete industries, report 562, center for by-products utilization. Milwaukee: The University of Wisconsin; 2005.
[2] Aïtcin P-C. Binders for durable and sustainable concrete. CRC Press; 2007. 528p.
[3] Caggiano A, Faella C, Lima C, Martinelli E, Mele M, Pasqualini A, et al. Mechanical behavior of concrete with recycled aggregate. In: 2nd Workshop on "The new boundaries of structural concrete", Università Politecnica delle Marche – ACI Italy Chapter, Ancona (Italy), 18–16 September 2011. p. 55–62.
[4] van Breugel K. Simulation of hydration and formation of structure in hardening cement-based materials. PhD thesis. Delft (Netherlands): Delft University of Technology; 1991. 171p.
[5] Bullard JW, Jennings HM, Livingston RA, Nonat A, Scherer GW, Schweitzer JS, et al. Mechanisms of cement hydration. Cem Concr Res 2011;41(12):1208–23.
[6] Koenders EAB. Simulation of volume changes in hardening cement-based materials. PhD thesis. Delft (Netherland): Delft University of Technology; 1997. 171p.
[7] Pane I, Hansen W. Investigation of blended cement hydration by isothermal calorimetry and thermal analysis. Cem Concr Res 2005;35(2005):1155–64.
[8] Lokhorst SJ. Deformation behavior of concrete influenced by hydration related changes of the microstructure, Internal Report Nr. 5-99-05. Delft (Netherland): Delft University of Technology; 1999.
[9] Gutsh AW. Properties of early age concrete – experiments and modelling. In: Proceedings int RILEM conference on early age cracking in cementitious systems; 2003. p. 11–18.
[10] Laube M. Werkshoffmodell jungen Betons. PhD thesis. TU Braunschweig; 1990.
[11] Krauss M, Hariri M, Rostásy F. In: Proceedings int RILEM conference on early age cracking in cementitious systems; 2003. p. 199–208.
[12] Livesey P, Donnelly A, Tomlinson C. Measurement of the heat of hydration of cement. Cem Concr Compos 1991;13(3):177–85.
[13] Brandštetr J, Polcer J, Krátký J, Holešinský R, Havlica J. Possibilities of the use of isoperibolic calorimetry for assessing the hydration behavior of cementitious systems. Cem Concr Res 2001;31(6):941–7.
[14] Feng X, Garboczi EJ, Bentz DP, Stutzman PE, Mason TO. Estimation of the degree of hydration of blended cement pastes by a scanning electron microscope point-counting procedure. Cem Concr Res 2004;34(10):1787–93.
[15] Jeong J, Zollinger D. Finite-element modeling and calibration of temperature prediction of hydrating Portland cement concrete pavements. J Mater Civ Eng 2006;18(3):317–24.
[16] Bentz DP. Three-dimensional computer simulation of Portland cement hydration and microstructure development. J Am Ceram Soc 1997;80(1):3–21.
[17] de Schutter G, Tearwe L. Degree of hydration-based description of mechanical properties of early age concrete. Mater Struct 1996;29(6):335–44.
[18] Schindler AK, Folliard KJ. Heat of hydration models for cementitious materials. ACI Mater J 2005;102(1):24–33.
[19] Narasimhan TN. Fourier's heat conduction equation: history, influence, and connections. Rev Geophys 1999;37(1):151–72.
[20] Koenders EAB. Mix design for venice barriers, Report Nr. 15.5-05-08, confidential communication; 2005.
[21] Van Breugel K. Concrete structures under temperature and shrinkage deformations. Lecture notes CT5120. TU Delft; 2004.
[22] Kada-Benameur H, Wirquin E, Duthoit B. Determination of apparent activation energy of concrete by isothermal calorimetry. Cem Concr Res 2000;30(2):301–5.
[23] D'Aloia L, Chanvillard G. Determining the "apparent" activation energy of concrete: Ea—numerical simulations of the heat of hydration of cement. Cem Concr Res 2002;32(8):1277–89.
[24] EN 197-1. Cement – composition, specification and conformity criteria – Part 1: Common cements; 2011.
[25] Gutsch A, Rostàsy FS. Young concrete under high tensile stresses – creep, relaxation and cracking. In: Proceedings of the RILEM symp thermal cracking in concrete at early ages, Munich; 1994, p. 111–8.
[26] de Schutter G. Applicability of degree of hydration concept and maturity method for thermo-visco-elastic behaviour of early age concrete. Cem Concr Compos 2004;26(5):437–43.
[27] Freiesleben-Hansen P, Pedersen EJ. Maturity computer for controlled curing and hardening of concrete. Nordic Concr Res 1977;1:21–5.
[28] Han N. Maturity method. In: Reinhardt HW, Grosse CU, editors, Advanced testing of cement-based materials during setting and hardening – final report of RILEM TC 185-ATC. RILEM Publications SARL; 2005. p. 277–96.
[29] Van Kan J, Segal A, Vermolen F. Numerical methods in scientific computing, department of applied mathematics. Delft University of Technology; 2008.
[30] Laube M. Werkstoffmodell zur Berechnung von Temperaturespannungen in massigen Betonbauteilen im jungem Alter, PhD-thesis, Braunschweig; 1991.
[31] Voglis N, Kakali G, Chaniotakis E, Tsivilis S. Portland-limestone cements. Their properties and hydration compared to those of other composite cements. Cem Concr Compos 2005;27(2):191–6.
[32] Wang X-Y, Lee H-S, Park K-B, Kim J-J, Golden JS. A multi-phase kinetic model to simulate hydration of slag–cement blends. Cem Concr Compos 2010;32(6):468–77.
[33] EN-12390-3. Testing hardened concrete. Part 3: Compressive strength of test specimens; 2009.
[34] Faella C, Martinelli E, Nigro E. Direct versus indirect method for identifying FRP-to-concrete interface relationships. ASCE J Compos Construct 2009;13(3):226–33.